NJC

Accepted Manuscript

This is an *Accepted Manuscript*, which has been through the Royal Society of Chemistry peer review process and has been accepted for publication.

Accepted Manuscripts are published online shortly after acceptance, before technical editing, formatting and proof reading. Using this free service, authors can make their results available to the community, in citable form, before we publish the edited article. We will replace this *Accepted Manuscript* with the edited and formatted *Advance Article* as soon as it is available.

You can find more information about *Accepted Manuscripts* in the Information for Authors.

Please note that technical editing may introduce minor changes to the text and/or graphics, which may alter content. The journal's standard Terms & Conditions and the Ethical guidelines still apply. In no event shall the Royal Society of Chemistry be held responsible for any errors or omissions in this *Accepted Manuscript* or any consequences arising from the use of any information it contains.

ROYAL SOCIETY OF CHEMISTRY

www.rsc.org/njc

NMR Study on the Gelation of N, N'-Bis (4-N-Alkylo-Xybenzoyl) Hydrazine (4Dn) in Two Aromatic Solvents

Jianxi Song,[a,b] Haitao Wang*[a] and Min Li*[a]

[a]Key Laboratory of Automobile Materials, Ministry of Education, Institute of Materials Science and Engineering, Jilin University, Changchun 130012, China

[b]Center of Analytical and Testing, Beihua University, Jilin 132013, China.

* Corresponding author

Tel: +86-431-85168254

E-mail: haitao_wang@jlu.edu.cn, minli@mail.jlu.edu.cn;

Abstract

Organogels that are self-assembled from simple gelators are an interesting class of nano- and mesoscale soft matter with simplicity and functionality. Investigating the precise roles of the organic solvents and their effects on stabilization of the formed organogel is an important topic for the development of low-molecular weight gelators. We found that thermal gel properties of the N, N'-Bis (4-N-Alkylo-Xybenzoyl) Hydrazine (4D16) is correlated with the Kamlet-Taft parameter and gain a detailed understanding of solvent role on gelation. Benzene and toluene are similar of aromatic solvents, but the varieties of physical characteristics of the 4D16 gels formed from these two solvents are large. We studied noncovalent force, association constant, and thermodynamic parameters of 4D16 aggregation process in these two aromatic solvents by NMR and explained why gelator 4D16 in toluene had a lower critical gelation concentration (CGC). We select 4D7 which has higher CGCs and its microstructures are similar to 4D16 in these two solvents to compare differences of solvents and find that gelator-solvent interaction can break up toluene oligomers, whereas this interaction does not disrupt benzene oligomers. The motion of gelator is restricted due to the defect size provided by the vicinity of the methyl groups in toluene oligomers, thus it is favorable for gelator-gelator interaction.

Keywords: N, N'-Bis (4-N-Alkylo-Xybenzoyl) Hydrazine; Noncovalent Force; Gelator-Solvent interaction; Association Constant; Thermodynamic Process

Introduction

Molecular gels represent an intriguing case of self assembly of low-molecular weight molecules (LMOGs) into nano(micro)fibrillar networks that percolate the solvent and transform it into a viscoelastic material, namely into a molecular gel.[1] The detailed rationalization of the structural, kinetic, and thermodynamic parameters relevant for aggregation processes that yield soft materials represents a very appealing goal.[2] In recent years, there has been great interest in gaining fundamental understanding of the thermodynamic and kinetic factors which control gelation[3] as only with a firm grip on these parameters will it be possible to design future soft materials with potential high-tech applications.[4] Key features of this type of soft matter when compared with most cases of gels formed by polymers are the remarkable lyo- and thermoreversibility together with the precise structural arrangement associated to the self-assembly process that generates molecular gels. These materials present applications in a wide range of areas such as optoelectronic materials, regenerative medicine, controlled drug release, or catalysts among others.[5] In addition, the interactions of solvent molecules with gelator during gelation, the influence of the gel matrix on the solvent dynamics, and the role of solvent after the gel formation, are still open for discussion. The solvent's influences on the physical properties of the gel after the gel formation are well documented in the literature.[6] Therefore, key information on gel assembly is needed with respect to gelation in different solvents to reveal the relationship between solvent-gelator interactions during gelation.

Among all of the spectroscopic techniques used to analyze the structure and understand self-assembly processes of molecular gels,[7] NMR spectroscopy is especially appealing. Correlation of variation of chemical shifts,[8] intensity of NMR signals with concentration, solvent composition and/or temperature,[9] analysis of NMR relaxation times[10] and diffusion spectroscopy are helpful to obtain information about intermolecular interactions, critical concentration values, the change in the motion of the molecules, the association constant and thermodynamic parameters

associated with the gel formation.

Previously, we reported the gel properties of N, N'-Bis (4-N-Alkylo-Xybenzoyl) Hydrazine (4D16) in benzene and toluene, respectively, through a range of techniques such as XRD, SEM, POM and time-dependent fluorescence emission spectroscopy.[11] However, deep understanding of the differences of the gelation in the two solvents are still inadequate. In this paper, we correlated the thermal properties of the gels with the Kamlet-Taft parameter.[12] Special attention was paid to the different influences of benzene and toluene on aggregation behavior of 4D16. In addition, we selected 4D7 which had relatively higher solubility in these two solvents to further explore the difference of benzene and toluene.

Results and Discussion

Scheme 1 shows the molecular structure of N, N'-Bis (4-N-Alkylo-Xybenzoyl) Hydrazine (4Dn) whose synthetic methods were reported previously,[13] and the labels of protons are also denoted. The 1D and 2D NMR spectra were recorded on Bruker Avance^{II} 500 MHz spectrometer using standard parameter settings.

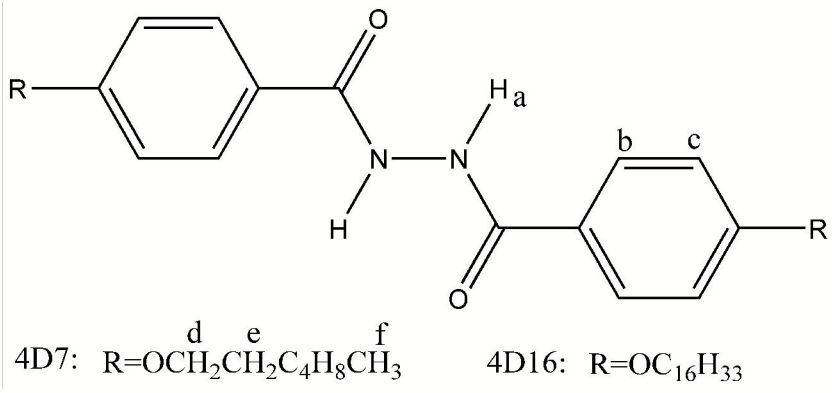

Scheme 1: Molecular structures of 4D16 and 4D7.

Solvent effects on gelation. We investigated the effect of solvent on 4D16 gelation. The macroscopic behavior of the obtained materials was initially analyzed by monitoring the transition from an immobile to a mobile aggregate state using "the tube inversion test". Then we attempt to correlate the critical gelation concentration (CGC) of 4D16 with a variety of solvent parameters.[14] We will find that the

Kamlet-Taft parameter[12] which has three parameters to describe different properties of a solvent (α=hydrogen bond donating ability, β= hydrogen bond accepting ability, and π* = polarizability) provides a better predictive correlation. Gels will form in solvents only when α is 0.00, therefore, it can be proposed that hydrogen bond donor solvents strongly inhibit gelation. The CGC values of the gels are plotted against the β and π* values for different solvent (Figure 1), however, it is not found that critical gelation concentration is correlated with any one of the parameters, while linear combination of these parameters gives rise to a good correlation (Figure 1) if β plus π*. Therefore, we conclude that the ability of solvent supporting gelation is not primarily dependent on its hydrogen bond donor (α)[14g] but is largely determined by the ability of solvent accepting hydrogen bonds (β) and its general polarity/polarizability (π*). If these values are much higher (e.g., in DMF, DMSO, etc.) then the soluble gelator will increase and thus there will be a higher CGC. In opposite, gelator will have a lower CGC in solvent (e.g., hexane) whose β and π* are much lower.

Figure 1. Correlation of CGC with Kamet-Taft parameters (β + π*),
■ corresponds to Hex, Pen, CYH, Et2O, DCE, EAC, THF, DMF, DMSO
from bottom to up, ● and ▲ correspond to PhMe and PhH, respectively.

The results show that both benzene and toluene have similar Kamlet-Taft

parameters whereas the CGC values of the gels formed in them are obviously different. In order to further explore the effect of solvent on gelation process, we will investigate the gelation behavior of 4D7 which has higher CGC in these two aromatic solvents.

Gelation of 4D7. Figure 2 shows plot of T_gs as a function of 4D7 concentration (mM). It can be seen that the T_gs increases with the increase of concentrations and 4D7 gel in toluene shows higher Tgs compared with that in benzene. Therefore, the 4D7 gel in toluene are more stable.

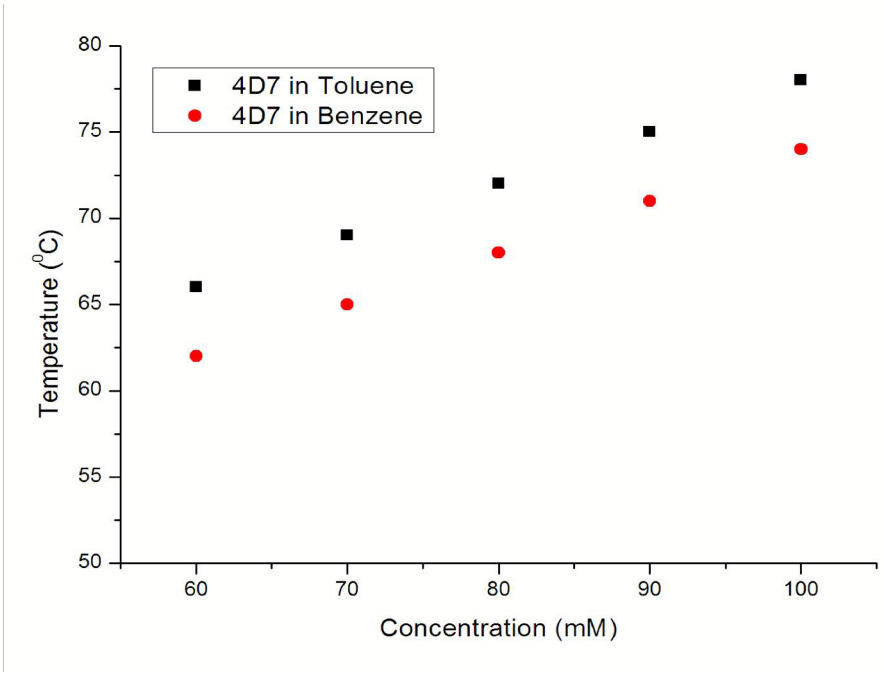

Figure 2. Plots of Tgs versus 4D7 concentration in benzene and in toluene.

SEM images of 4D7 xerogels are shown in Figure 3. It can be seen that different behaviors of self-aggregation of 4D7 in benzene and toluene are also reflected in different microstructures of gels which have been studied. The SEM image of 4D7 xerogel formed in benzene shows that the approximately 0.5μm diameter fiber is the constitutional unit, which are bundled together to make thicker fibers and they cross and stick together to form radial broom-like shape; while the xerogel formed in toluene shows that bundles of rods with the width of roughly 1μm, relatively short, have proximately average apparent density and different orientations. The microstructure differences of 4D16 xerogel[11] formed in these two solvents are

similar to those of 4D7 xerogel. Therefore, these structural features are determined by the extent of the solvent-gelator interactions. Usually, rod-like fibers forming three-dimensional sponge-like network can efficiently entrap a solvent by capillary forces and surface tension.[15] Compared the SEM images of these two gels (figure 3), 4D7 xerogel formed in toluene is relatively favorable to entrap solvent because rod-like fibers which possess proximately average apparent density can produce larger specific surface area.

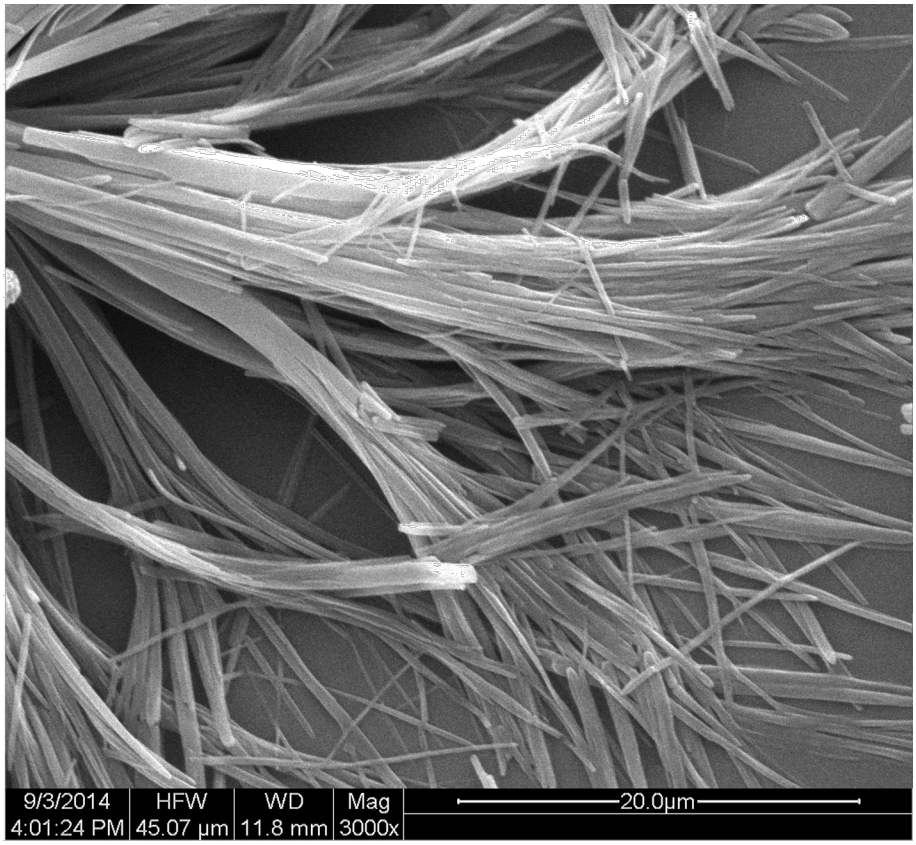

Figure 3. SEM images of the xerogels of 4D7 (50mM)
from benzene (up) and from toluene (down).

D**riving force for the self-assembly** In order to identify the noncovalent interactions during gelation, Temperature-dependent NMR measurement of 4D16 (24 mM) was performed in toluene-d_8 and benzene-d_6, respectively.

Figure 4. Superimposition of 4D16 (24 mM) ^{1}H NMR spectra recorded
in toluene-d_8 at different temperatures.

Figure 4 shows the ^{1}H NMR spectra of 4D16 in toluene-d_8 (24 mM) at different temperatures. Obviously, NH peak of the amide group of 4D16 exhibits a significant shift with the temperature decreasing, e.g. there is a downfield shift when the temperatures are higher than 338K, which suggests an intermolecular hydrogen bonding between amide groups is the driving force for the self-assembly of 4D16. In opposite, there exhibits a gradual upfield shift when the temperatures are lower than 338K. The distinct decrease of NH chemical shift is observed at 337K in toluene-d_8 and at 333K in benzene-d_6 (figure s1), respectively. The different chemical shift tendency is attributed to the change of solubility in the lower temperature range, within which decrease of temperature has caused the decrease of solubility so as to weaken the hydrogen bonding, while temperature decreasing will also strengthen the hydrogen bonding. The above two opposite effect of temperature decrease resulted in the present chemical shift with temperature. Interestingly, chemical shift displacement of aromatic proton (Ar-H_b) is similar to that of amide proton (NH) while that of aromatic proton (Ar-H_c) displays little changes with temperature in aromatic solvents. Usually, aromatic protons shows upfield shift with the temperature decreasing due to the influence of the ring current from the neighboring molecule.[16] Therefore, these observations indirectly indicate that the NMR signals observed with temperature reduction are consistent with the associated molecules via hydrogen bonding interactions,[17] and the solvent molecules effectively solvate the solute and influence hydrogen bonding strength during the aggregation.

NMR spectra of 4D16 with a total concentration of 24mM at different temperatures were measured by using diphenylmethane as internal standard to quantify soluble molecules within the sample in toluene-d_8 and benzene-d_6, respectively (figure 4 and figure s1). We define 4D16 as soluble if its signals of protons are visible by NMR and define it as insoluble aggregates if they are not. On decreasing the temperature, the amount of soluble gelator decreases as the gelator gradually aggregate.

This study allows a number of parameters to be experimentally determined: [18] they are the temperature at which the gelator network begins to aggregate (T_b) and the

amount of the insoluble gelator complex (i.e., within the fibers) at the T_g value ([Insol]@T_{gel}). In these two cases, the higher T_g value corresponding to the higher T_b value (Table 1) indicates that what is observed macroscopically on breakdown of the gel (T_g) reflects what is happening at the molecular scale in terms of gelator aggregation. The value of T_g is slightly lower than that of T_b as it represents the point at which the gel network is partly dissolved and the remaining sample-spanning gel network becomes unable to self-support, whereas T_b is the temperature at which the solution starts to have aggregates. The [Insol]@T_{gel} of each sample is compared with the CGC values. The former indicates how much network is needed to ensure the sample could support itself against gravity, whereas the latter is the minimum total concentration of gelator required to form a stable gel which can immobilize the solvent at ambient temperature.

Table 1[a]. Correlation between Macroscopic Observations of Gels (T_{gel} and CGC Values) and NMR Molecular-Scale Parameters (T_b and [Insol]@Tgel)

	Macroscopic observation		Molecular-scale parameters from NMR	
	T_{gel} (K)	CGC (mM)	T_b (K)	[Insol]@T_{gel} (mM)
4D16 in Tol	334	14	337	19.33
4D16 in Ben	331	21	333	19.52

[a] Except for CGC, all calculated parameters were based on 24mM 4D16.

As we expected, the 4D16 gel formed in toluene has a lower CGC and a higher T_g and T_b compared with that in benzene. However, the [Insol]@T_{gel} value of 4D16 gel formed in toluene and that in benzene are identical, i.e., the amount of gelator required to form a fibrillar solidlike state which can support itself against gravity at the gel-sol transformation temperature in toluene is equal to that in benzene. This suggests that the fibre structures formed in these two solvents are different because only different fibre structures formed from the same amount of gelator at different temperature can they support itself against the same gravity. Therefore, comparing two gels, 4D16 gel formed in toluene is relatively more stable because its [Insol]@T_{gel} value is at the higher temperature. In addition, comparing two T_bs, the higher T_b suggests that gelator 4D16 in toluene is more favorable to form gel fibre.

Then we applied a van't Hoff treatment to the VT NMR data and to investigate

the aggregation process during fiber formation.[19] It can be seen that the spectral resolution decreased compared with the fixed intensity of the internal standard (CH_2, diphenylmethane) with the decrease of temperature (figure 4). The amount of gelator observed by ^1H NMR is significantly lower than the actual amount below the T_b indicating that some gelator are being incorporated into the NMR-silent aggregates. Therefore, in this case, the concentration corresponds to maximum solubility of the gelator with the temperature decreasing and can be considered to be the saturation point of this system below the T_b. For an ideal solution, the solubility (Sol) at a given temperature can be expressed by the van't Hoff equation:

$$\mathrm{Ln(Sol)} = (-\Delta H/RT) + (\Delta S/R)$$

ΔH and ΔS denote the molar enthalpy and the molar entropy for the dissolution process (i.e, gel-sol transformation), T is the equilibrium temperature, and R is the gas constant. A typical van't Hoff plot for one of the systems under investigation **(4D16)** is shown in Figure 5. A similar analysis is also performed in this study for 4D16 at the same concentration (24mM) in benzene and in cyclohexane, respectively (data not shown). This plot can be used to calculate ΔH and ΔS, and furthermore, extrapolation of this data permits the solubility (i.e., the amount of gelator in the liquidlike phase) at different temperatures to be determined. Data are collected in the range of 298-333K, and the assumption is made that ΔH and ΔS are temperature independent. Given that NMR provides a direct measure of "solubility", this approach allows thermodynamic parameters associated with gelation/dissolution to be extracted (table 2).

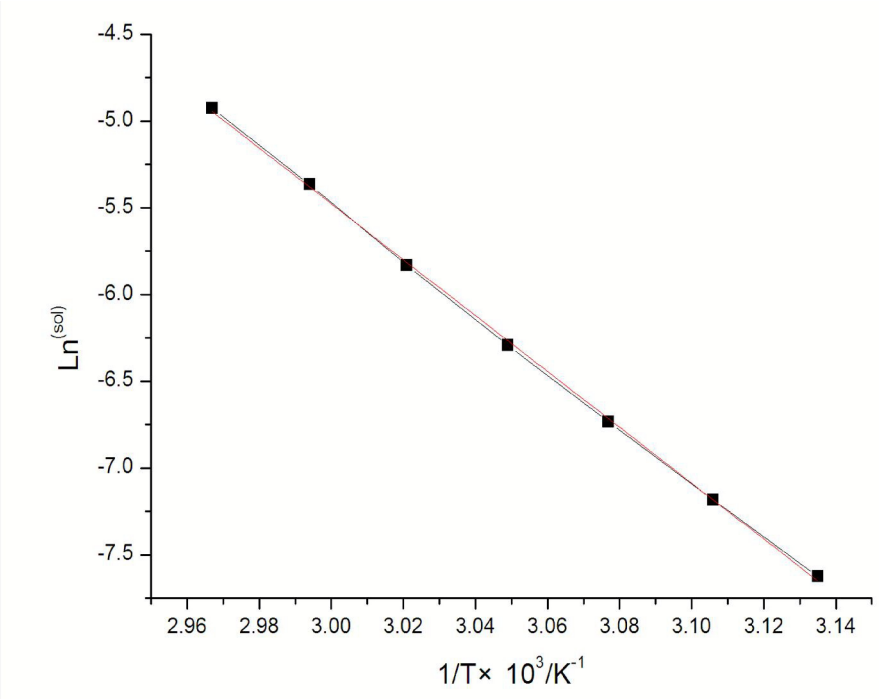

Figure 5. Plot of $\ln^{Sol}$ (Sol=solubility, i.e., the concentration of gelator species in solution) against the reciprocal of the dissolution temperature for **4D16** in toluene.

Table 2. Thermodynamic Parameters Extracted from the van't Hoff Treatment of VT NMR Data in the Temperature Range 298-333K.

	-△H KJ·mol^{-1}	-△S J·mol^{-1}·K^{-1}	-△G KJ·mol^{-1}
4D16 in Tol	-133.77	-355.80	-27.74
4D16 in Ben	-138.01	-372.13	-27.11
4D16 in Cyclohexane	-171.27	-435.82	-41.39

As can be seen from table 2, gelation (which is the inverse of the dissolution process) is enthalpically favorable and entropically disfavored as would be expected for the assembly of ordered fibers through hydrogen bonding interaction. Hydrogen bond accepting ability and polarizability of aprotic solvent (table s1) have a profound effect on the sol-gel gelation thermodynamic process. The enthalpy of gelation, ΔH, increases about 45 kJ mol^{-1} from in aromatic solvent to in cyclohexane, confirming that the aggregation of 4D16 in cyclohexane is favorable for intermolecular forces. 4D16 in cyclohexane also confers a higher degree of order in the self-assembled fibrillar network as demonstrated by the fact that much more entropy is released.

4D16 in cyclohexane makes the ΔG value much more negative than that in aromatic solvents at 298 K, and the ΔG value in toluene is more negative than that in benzene, suggesting that the aggregation of 4D16 in toluene is more stable than that in

benzene and 4D16 in cyclohexane is more facile to aggregate.

The above treatment suggests that the hydrogen bond accepting ability and polarizability of aprotic solvent modify the gel-sol dissolution process by (i) π electrons of aromatic solvent forms p-π hydrogen bond with 4D16 and this hydrogen bond strength is related to hydrogen bond accepting ability of aromatic solvent. (ii) polarizability of aprotic solvent produces induction force with 4D16 and its strength is related to polarizability magnitude. The interaction between solvent and solute enhance solubility of 4D16 in aromatic solvents, but reduce interaction between gelators. As a result, this higher solubility reflects the lower enthalpic cost compared with that of 4D16 in cyclohexane, underlining the important role of solvent on the gelator aggregation.

Association constant. The experimentally determined NMR shifts as a function of the concentration of 4D16 were used in the aggregation models to estimate the association constants[20] at 338K in toluene and benzene, respectively, because there are no aggregates at this temperature (nonaggregated state, observable by NMR). Here, two models were used, and the constants in the models were fitted to experimental data using nonlinear least-squares fitting. All models are based on the assumption that the chemical shift of an oligomer can be expressed in terms of those of the monomer, a molecule at the end of a stack, a molecule within a stack, and their respective concentrations. The equal K (EK) model assumes that the addition of a molecule to a stack occurs with the same equilibrium constant as other molecules. These models assume that only nearest-neighbor interactions produce chemical shifts and they can be extended to account for the interactions of next-nearest-neighbors (EKNN). A summary of parameters determined using the different models for the curve-fitting are given in Table 3. The experimental data agree well with the fitting. The association constants are $200M^{-1}$ in toluene and 400 M^{-1} in benzene at 338K, respectively. These values are much higher than those of gelators with lysine units[19a] in the similar solvent. This difference in magnitude certainly can be explained by several reasons: they are the elevated temperature which is utilized in this experiment

(according to the van't Hoff law), the more polar solvent which is selected there (for solubility reasons) and the highly simplified model where higher aggregates are neglected is used by them.

The above experimental results show that the K_E in benzene is approximately twice that of in toluene and $\rho>1$ by either EK model or EKNN model to calculate equilibrium constant. Usually, if $\rho>1$, the formation of dimer is more easily than subsequent additions,[20] indicating that 4D16 in benzene is more facile to form dimer at first. Jeffrey S. Moore also hold the same view that if K_2 is larger than the equilibrium constants of the remaining steps, the system experiences tight dimerization followed by isodesmic elongation.[21] Besides, the temperature of forming insoluble 4D16 aggregates (aggregated state, NMR-silent) in benzene is lower than that in toluene at the same concentration of gelators (figure 4 and figure s1). These indicate that oligomers of 4D16 in benzene at 338K are mainly dimers; while that in toluene at this temperature have more multimers, i.e., the gelator molecules have formed sufficient network and are about to further form sample-spanning gel network which can immobilize the solvent, therefore, it is more facile to form organogel.

Table 3. Parameters for the Different Models Using the Entire Set of experimental Data[a] by fitting the dilution curves at 338 K.

	EK model			EKNN model	
	4D16 in Tol	4D16 in Ben		4D16 in Tol	4D16 in Ben
K_E	200.0009	400.0004	K_E	199.9931	399.8979
ρ	1.000265	1.254915	ρ	1.000111	2.270374
f	0.10368	0	r	1	1
P_m	8.5	8.824622	P_m	8.5	8.597671
P_a	10.5	10.3	P_a	10.1659	10.3

a K_E, equilibrium constant; ρ, factor by which dimer formation differed from larger aggregate formation in EK models ($K2=\rho KE$); f, factor relating the shift of the terminal molecule in the aggregate to that of the monomer and the interior molecule ($P\lambda=(1-f)\ P_m + f\ P_a$); P_m, NMR chemical shift of monomer; P_a, NMR chemical shift of the interior molecule. Detailed explanations of these models were presented in ref.[20]

The precise position. 4D7 in chloroform is dissoluble and its VT-NMR study shows that as the temperature of the sample (50mM) was decreased (figure s2), the

NH peak of the amide group shifting downfield and aromatic protons shifting upfield are consistent with aggregation of 4D7 by intermolecular hydrogen bonding between the amide groups and π-π interaction between the aromatic groups. In order to study the interaction between aromatic solvent and the position of proton in molecular, the aromatic solvents toluene-d_8 and benzene-d_6, respectively, were added into $CDCl_3$ solution of 4D7 (the concentration of gelator 4D7 is always 8.1mM in each mixture solvent), which caused the changes in the ^1H chemical shifts of some signals.

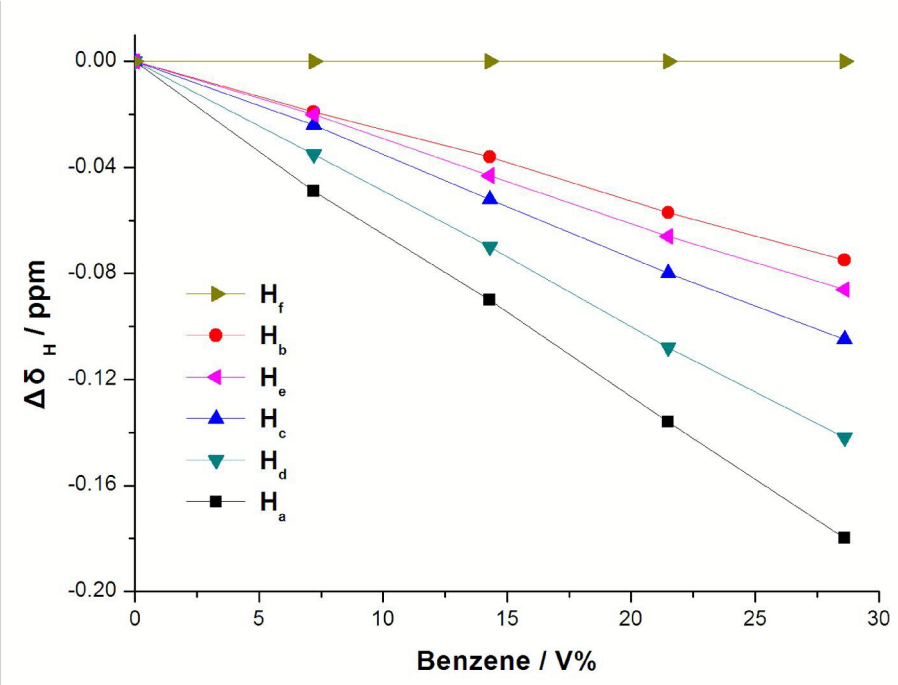

Figure 6. Peak shifts with various volume percentages of aromatic solvents in aromatic solvents/chloroform-d_1 mixture solvents for 4D7 (8.1mM).

Figure 6 shows the changes in the ^{1}H chemical shifts with the volume percentages of benzene-d_8 in the benzene-d_8/chloroform-d_1 mixtures for 4D7. Unexpectedly, almost all the chemical shifts are decreased with increasing fraction of the aromatic components. In general, the chemical shift of proton participating in hydrogen bonding shifts downfield and that participating in π-π interaction shifts upfield with aggregation of gelator. The larger the $|\Delta\delta_H|$ is, the stronger the strength of intermolecular interaction is.

The $|\Delta\delta_H|$ of 4D7 decrease in the sequence H_a, H_d, H_c, H_e, H_b, H_f, indicating that intermolecular interaction between alkyls (from H_d to H_f) is decreased when the distance of alkyl protons from aromatic ring becomes large; The $|\Delta\delta|$ of aromatic proton H_b is smaller than that of alkyl H_e, which shows that aromatic solvents significantly reduce π-stacking interactions because π-π interaction between aromatic protons is usually stronger than alkyl protons. However, the signal of amide proton (Ha) shifting upfield is beyond our expectation because the proton signal of amide also shifts downfield with cyclohexane component increasing in cyclohexane/chloroform-d_1 mixture solvent (figure s3). While gelator 4D7 is aggregating, the amide proton forms intermolecular hydrogen bonding and shifts

downfield; whereas amide protons of 4D7 in aromatic solvents forms p-π hydrogen bonding with π electrons of solvent and shifts downfield; amide protons is in the shield area of aromatic solvent and shifts upfield at the same time. This phenomenon that the residual chloroform proton signal of chloroform-d_1 in toluene-d_8/chloroform-d_1 mixture solvents shifts upfield with the proportion of the toluene-d_8 increasing can be observed. Therefore, the chemical shift of the amide proton (H_a) exhibits upfield because the latter is predominant. This result indicates that there is an interaction between aromatic solvent and amide proton. Similar results are also acquired in toluene-d_8/chloroform-d_1 mixture solvent, but the displacement of amide proton chemical shift is relatively smaller than that in benzene-d_6/ chloroform-d_1 (figure S2), which suggests that the interaction between toluene and amide proton is relatively weaker compared with the interaction between benzene and amide proton.

The precise role of the organic solvent in gelating and determining the macroscopic properties of the gel should also be considered because the formation of organogels is both the result of gelator-gelator interaction and solvent-gelator interaction.[22] If solvent-gelator interaction is too strong then the gelator will become too soluble to assemble and it will dissolve instead, while if this interaction is too weak, the gelator will be too insoluble to form gel networks within the solvent phase and it will form precipitate. So gelator-gelator interaction is the strongest in a solvent that has minimum interaction with the gelator, which prefers the formation of fine nanofibers. Therefore, the interaction between aromatic solvent and amide proton is the reason that gelator 4D7 has a relatively higher CGC in these two aromatic solvents and the CGC of gelator 4D7 in toluene is much lower than that in benzene.

Diffusion of benzene and toluene solvents in the presence of gelator 4D7. The conventional pulse gradient spin echo (PGSE) methodology has been successfully applied in the observations of diffusion behavior of solvent molecules entrapped in gel phase.[23] Here, we investigated the solvent diffusion in the presence of gelator 4D7 from benzene and toluene. The connection between diffusion (D) and structural

property arises because diffusion coefficient depends on friction factor (f_T) which is related to the molecular size and the viscosity of the solution: $D=k_BT/f_T$, where k_B is the Boltzmann constant and T is the absolute temperature. Several models can be used to calculate the friction factors, in which molecules are considered as ellipsoids, spheres or collections of spherical subunits. In the special case of a spherical molecule of hydrodynamic radius r_H in a solvent of viscosity η, the diffusion can be described according to the Stokes-Einstein equation: $D= k_BT/6\pi\eta r_H$.[24] Since a modification of the solution composition is expected to induce the change in the viscosity, and gives the fact that this change affects equally all compounds in the solution. The measured diffusion coefficients (D) of benzene and toluene shows the dependence on both gelator concentration and diffusion time Δ (Figure 7). They are estimated with the same analysis.[25]

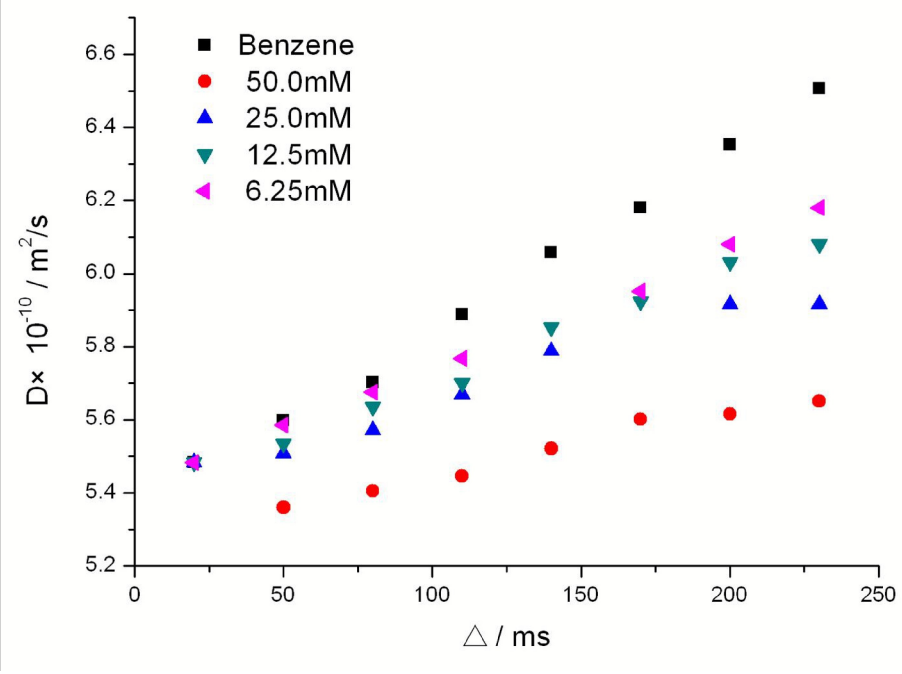

Figure 7. The diffusion coefficients D of benzene (up) and toluene (down) as a function of the diffusion time Δ and gelator concentration.

For all of the samples tested, the diffusion coefficients (D) increase with diffusion times increasing (from 20ms to 230 ms), although the magnitude of the change is different. The plots in Figure 7 show that the diffusion coefficient of toluene is similar to that of pure benzene, because their viscosity values are similar, e.g. 0.638 mPa·S at 20°C for benzene and 0.580 mPa·S for toluene.

The diffusion coefficients of benzene and toluene in the presence of gelator 4D7 increase and show a similar Δ dependence. In contrast, the diffusion coefficients of benzene and toluene in the presence of gelator 4D7 decrease with the increasing of gelator concentration. The lower values of D in gels compared with the pure solvent are indicative of the restricted diffusion of benzene and toluene inside the pore spaces of the corresponding gel matrixes of 4D7.

It is interesting to compare the D values for benzene and toluene, respectively, if there exists 6.25mM gelator with corresponding values for bulk solvents. The former is close to that of the bulk benzene, whereas the latter is faster than that of the bulk toluene. It is well established that the increase of gelator concentration leads to the decrease of diffusion mobility of solvent. Therefore, the behavior observed for toluene is somehow intriguing. This provides us with an interesting question: why is the

diffusion coefficient of the solvent faster than bulk pure toluene when the gelator concentration is 6.25mM, i.e., why does the existence of a small amount of gelator accelerate the diffusion of toluene?

We postulate that the explanation of this is connected to the molecular structure of the solvent. Toluene has a methyl group. Therefore, in the toluene oligomers formed by π-π interaction, the vicinity of the methyl groups in the oligomers can provide the needed defect size, which is necessary to make it possible for the interaction of gelator with the toluene molecules. As a consequence of gelator-solvent interaction, a dynamic oligomers of toluene is disrupted or broken down to some extent, which means that hydrodynamic radius (r_H) of toluene oligomers have reduced. At the same time, the viscosity (η) of solution increases with further increase of gelator concentration. If the product of solution for r_H and η at the lower gelator concentration (6.25 mM) is lower than that of the corresponding bulk toluene solvent, it will accelerate the diffusion of toluene. At relatively higher concentration of gelator, the increasing of viscosity is predominant so that the diffusion of toluene decreases. Similar results are also acquired by Cabrita and Berger.[26] They studied the diffusion of 2,6-di-tert-butylphenol in the presence of a small amount of hexamethylphosphoramide and found that it accelerates because some oligomers of 2,6-di-tert-butylphenol are disrupted when there is a small number of hexamethylphosphoramide.

In contrast to toluene, for the oligomers of benzene, it does not have any methyl. Therefore, there are no defect sizes in the oligomers, the effective solvent size is large, and gelator aggregates have difficulties inserting into such a network and disrupting it.

These results suggest that the motion of gelator is restricted due to the defect size provided by the vicinity of the methyl groups in toluene oligomers and this is favorable for gelator-gelator interaction. In benzene, however, the formation of organogels is the normal competition between gelator-gelator interaction and solvent-gelator interaction. Therefore, the former is more conducive to form the organogel than the latter. This conclusion may also explain why 4D16 in

methycyclohexane has a much lower CGC than that in cyclohexane (table s1).

Conclusions

In this paper, we have been demonstrated that the thermal gel properties of the N, N'-Bis (4-N-Alkylo-Xybenzoyl) Hydrazine (4D16) is correlated with the Kamlet-Taft parameter. Benzene and toluene are similar of aromatic solvents, with similar chemical formulas and molecule shapes. However, the critical gelation concentration (CGC) and gel microstructure formed in these two solvents have obvious differences.

Temperature-dependent NMR measurements indicate that the main noncovalent force that underpins gelation process in these two aromatic solvents is hydrogen bonding and chemical shift of amide proton shift upfield because solubility of gelator 4D16 decreases with the decrease of temperature. Thermodynamic study also shows that the gel stability of 4D16 formed in toluene is more stable than that in benzene and solvent properties effect the thermodynamic process while the gelator is aggregating. In addition, comparing the amount of the insoluble gelator complex (i.e., within the fibers) at the T_g value in these two solvents also displays that the fibre structure formed in toluene is more stable. The calculation of association constant demonstrates that 24mM gelator 4D16 in toluene have formed sufficient network and are about to further form sample-spanning gel network which can immobilize the solvent at 338K; while the same amount of gelator in benzene at this temperature still exists in the form of dimers.

The method of mixture solvent indicates that there is an interaction between aromatic solvent and amide proton and this interaction in benzene makes amide proton have large chemical shift change, which leads to the CGC of gelator 4D7 is much higher than that in toluene. The DOSY measurement suggests that the motion of gelator is restricted due to the defect size provided by the vicinity of the methyl groups in toluene oligomers and this is favorable for gelator-gelator interaction.

In the molecular gels, the question about the solvent-gelator interaction is one of the most important and still open for discussion. We believe that the presented results shed new light on this interaction. The interesting results concern the solvent effect.

The studies presented have shown that even the same type of solvent, aromatic solvents, can also affect in a different way the aggregation mode of the same gelator and consequently further the properties of gel.

Experimental section

Gel Preparation. Organogels were prepared by dissolving a weighted amount of gelator with solvent in a sealed test tube and the mixture was then heated until the solid was completely dissolved. The solution was set aside and allowed to cool to room temperature. Gelation was considered to occur when the tube could be turned upside down without fluid dripping out.

Determination of the Gel-Sol Phase Transition Temperature (Tgs). The temperature was determined by using the reproducible and simple tube-inversion method.

Scanning Electron Microscopy. SEM observations were taken by FEI Quanta 200 (America). Samples for SEM observation were prepared by placing a drop of hot solution on silicon slides and then immediately dried

Solubility Analysis. ^{1}H NMR spectra of the gels were used to estimate the solubility constants at different temperatures. The measurements were recorded at the desired temperature after stabilization for 2 minutes. The relative integral value of the aromatic protons to the internal standard was measured. The results were reproduced successfully at least twice.

NMR Diffusion Experiment. NMR diffusion measurements were performed on a Bruker Avance^{II} spectrometer with BBO probe operating at 500 MHz for protons. The capillary tubes filled with D_2O were inserted to 5 mm NMR tubes which were used for these measurements because D_2O was needed to lock and to be as the external reference.

Longitudinal eddy current delay and bipolar gradients (ledbpgs2s) pulse sequence was applied for measuring diffusion of pure solvents and solvents confined in gelator mixtures. The signal is phase encoded according to the molecular displacement over a Δ diffusion time. The molecular displacement leads to an

attenuation of the echo signal, which is related to the experimental parameters by Stejskal-Tanner relation.

$$\ln(I/I_0)=-(\gamma G\delta)^2 D(\Delta-\delta/3)$$

where I and I_0 are echo signal intensities with and without magnetic field gradient pulse applied, γ is the gyromagnetic ratio of the nucleus studied, and D is the self diffusion coefficient. The echo signal intensity was measured as a function of g.

In our experiment, the pulse gradient was applied in the z direction and varied in 32 steps from 0 to a maximum value. The gradient duration δ was equal to 2 ms. The diffusion coefficients for bulk benzene & toluene solvents and these solvents in gelator concentration from 6.25mM to 50mM were studied as a function of Δ in the range from 20 to 230 ms at 293K.

Acknowledgment. The authors are grateful to the National Science Foundation Committee of China (Project Nos. 51073071, 21072076 and 51103057), and Project 985-Automotive Engineering of Jilin University for financial support of this work.

†Electronic Supplementary Information (ESI) available: [Table S1, Fig.S1-S3]. See DOI: 10.1039/b000000x/

References

[1] (a) R. G. Weiss and P. Terech, Molecular Gels: Materials with Self-Assembled Fibrillar Networks, Springer, Heidelberg, 2005; (b) F. Fages, Low Molecular Mass Gelators, Springer, Heidelberg, 2005; (c) P. Terech and R. G. Weiss, *Chem. Rev.*,1997, **97**, 3133; (d) D. J. Abdallah and R. G. Weiss, *Adv. Mater.*, 2000, **12**, 1237; (e) J. H. van Esch and B. L. Feringa, *Angew. Chem.* 2000, **112**, 2351; (f) A. R. Hirst and D. K. Smith, *Chem. Eur. J.*, 2005, **11**, 5496; (g) J. W. Steed, *Chem. Commun.*, 2011, **47**, 1379.

[2] (a) D. F. Evans and H. Wennerstrom, The Colloidal Domain: Where Physics, Chemistry, Biology, and Technology Meet, WILEY-VCH, Weinheim, **1999**; b) I. W. Hamley, Introduction to Soft Matter: Polymers, Colloids, Amphiphiles and Liquid Crystals, Wiley, New York, **2000**.

[3] (a) P. Jonkheijm, P. van der Schoot, A. P. H. J. Schenning and E. W. Meijer, *Science*, 2006, **313**, 80-83; (b) X. Huang, P. Terech, S. R. Raghavan and R. G. Weiss, *J. Am. Chem. Soc.*, 2005, **127**, 4336-4344; (c) X. Y. Liu and P. D. Sawant, *Adv. Mater.*, 2002, 14, 421. (d) X. Huang, S. R. Raghavan, P. Terech and R. G. Weiss, *J. Am. Chem. Soc.*, 2006, **128**, 15341-15352; (e) M. L. Muro-Small, J. Chen and A. J. McNeil, *Langmuir*, 2011, **27**, 13248-13253.

[4] (a) S. Banerjee, R. K. Das and U. J. Maitra, *J. Mater. Chem.*, 2009, **19**, 6649-6687; (b) A. R. Hirst, B. Escuder, J. F. Miravet and D. K. Smith, *Angew. Chem. Int. Ed.*, 2008, **47**, 8002-8018.

[5] (a) A. R. Hirst, B. Escuder, J. F. Miravet and D. K. Smith, *Angew. Chem.*, 2008, **120**, 8122-8139; (b) B. Escuder, F. RodrÝguez-Llansola and J. F. Miravet, *New J. Chem.*, 2010, **34**, 1044-1054.

[6] (a) M. Bielejewski, J. Kowalczuk, J. Kaszyńska, A. Łapiński, R. Luboradzki, O. Demchuk, *Soft Matter*, 2013, **9**, 7501-7514; (b) J. Kaszyńska, A. Łapiński, M. Bielejewski, R. Luboradzki, J. Tritt-Goc, *Tetrahedron*, 2012, **68**, 3803-3810.

[7] L. A. Estroff and A. D. Hamilton, *Chem. Rev.*, 2004, **104**, 1201-1217.

[8] (a) Y. Chen, Y. Lv, Y. Han, B. Zhu, F. Zhang, Z. Bo and C. Y. Liu, *Langmuir*, 2009, **25**, 8548-8555; (b) S. Debnath, A. Shome, S. Dutta and P. K. Das, *Chem. Eur. J.*, 2008, **14**, 6870-6881; (c) S. R. Nam, H. Y. Lee and J. I. Hong, *Tetrahedron*, 2008, **64**, 10531-10537; (d) K. M. Sureshan, K. Yamaguchi, Y. Sei and Y. Watanabe, *Eur. J. Org. Chem.*, 2004, 4703-4709; (e) J. Makarevic, M. Jokic, Z. Raza, Z. Stefanic, B. Kojic-Prodic and M. Zinic, *Chem. Eur. J.*, 2003, **9**, 5567-5580; (f) J. H. Jung, S. Shinkai and T. Shimizu, *Chem. Eur. J.*, 2002, **8**, 2684-2690.

[9] (a) S. K. Samanta, A. Pal and S. Bhattacharya, *Langmuir*, 2009, **25**, 8567-8578; (b) P. C. Xue, R. Lu, G. J. Chen, Y. Zhang, H. Nomoto, M. Takafuji and H. Ihara, *Chem. Eur. J.* 2007, **13**, 8231-8239; (c) V. Kral, S. Pataridis, V. Setnicka, K. Zaruba, M. Urbanova and K. Volka, *Tetrahedron*, 2005, **61**, 5499-5506; (d) D. Rizkov, J. Gun, O. Lev, R. Sicsic and A. Melman, *Langmuir*, 2005, **21**, 12130-12138; (e)K. Sakurai, Y. Jeong, K. Koumoto, A. Friggeri, O. Gronwald, S. Sakurai, S. Okamoto, K. Inoue and S. Shinkai, *Langmuir*, 2003, **19**, 8211-8217.

[10] (a) M. Bielejewski, A. Rachocki, R. Luboradzki and J. Tritt-Goc, *Appl. Magn. Reson.*, 2008, **33**, 431-438; (b) J. Tritt-Goc, M. Bielejewski, R. Luboradzki and A. Lapinski, *Langmuir*, 2008, **24**, 534-540; (c) M. George and R. G. Weiss, *Langmuir*, 2003, **19**, 8168-8176; (d) D. C. Duncan and D. G. Whitten, *Langmuir*, 2000, **16**, 6445-6452; (e) G. Cassin, C. de Costa, J. P. M. van Duynhoven and W. G. M. Agterof, *Langmuir*, 1998, **14**, 5757-5763; (f) D. Capitani, L. Segre, F. Dreher, P. Walde and P. L. Luisi, *J. Phys. Chem.*, 1996, **100**, 15211-15217; (g) M. Tata, V. T. John, Y. Y. Waguespack and G. L. McPherson, *J. Phys. Chem.*, 1994, **98**, 3809-3817; (h) D. Capitani, E. Rossi and A. L. Segre, *Langmuir*, 1993, **9**, 685-689.

[11] Y. Zhang, H. T. Wang, C. X. Zhao, B. L. Bai and M. Li, *Soft Materials*, 2014, **12**, 230-236.

[12] M. J. Kamlet, J. L. M. Abboud, M. H. Abraham and R. W. Taft, *J. Org. Chem.*, 1993, **48**, 2877-2887.

[13] H. Xin, X. M. Zhou, C. X. Zhao, H. T. Wang and M. Li, *J. Mol. Liquid*, 2011, **160**, 17-21.

[14] (a) A. R. Hirst and D. K. Smith, *Langmuir*, 2004, **20**, 10851-10857; (b) K. Hanabusa, M. Matsumoto, M. Kimura, A. Kakehi and H. Shirai, J. Colloid Interface Sci., 2000, **224**, 231-244;

(c) G. Zhu and J. S. Dordick, *Chem. Mater.* 2006, **18**, 5988-5995; (d) M. Bielejewski, A. Lapinski, R. Luboradzki and J. Tritt-Goc, *Tetrahedron*, 2011, **67**, 7222-7230; (e) M. A. Rogers and A. G. Marangoni, *Langmuir*, 2009, **25**, 8556-8566; (f) M. Raynal and L. Bouteiller, *Chem. Commun.*, 2011, **47**, 8271-8273; (g) W. Edwards, C. A. Lagadec and D. K. Smith, *Soft Matter* , 2011, **7**, 110-117; (h) Y. P. Wu, S. Wu, G. Zou and Q. Zhang, *Soft Matter*, 2011, **7**, 9177-9183; (i) H. Q. Xu, J. Song, T. Tian and R. X. Feng, *Soft Matter*, 2012, **8**, 3478-3486; (j) S. J. Liu, W. Yu and C. X. Zhou, *Soft Matter*, 2013, **9**, 864-874.

[15] P. Terech, I. Furman and R. G. Weiss, *J. Phys. Chem.*, 1995, **99**, 9558-66.

[16] A. S. Shetty, J. S. Zhang and J. S. Moore, *J. Am. Chem. Soc.*, 1996, **118**, 1019-1027.

[17] (a) V. Kral, S. Pataridis, V. Setnicka, K. Zaruba, M. Urbanova and K. Volka,

Tetrahedron, 2005, **61**, 5499-5506; (b) B. Huang, A. R. Hirst, D. K. Smith, V. Castelletto and I. W. Hamley, *J. Am. Chem. Soc.*, 2005, **127**, 7130-7139; (c) F. S. Schoonbeek, J. V. van Esch, R. Hulst, R. M. Kellogg and B. L. Feringa, *Chem. Eur. J.*, 2000, **6**, 2633-2643. (d) J. Makarevic, M. Jokic, Z. Raza, Z. Stefanic, B. KojicProdic and M. Zinic, *Chem. Eur. J.*, 2003, **9**, 5567-5580.

[18] W. Edwards and D. K. Smith, *J. Am. Chem. Soc.*, 2013, **135**, 5911-5920.

[19] (a) A. R. Hirst, I. A. Coates, T. R. Boucheteau, J. F. Miravet, B. Escuder, V. Castelletto, I. W. Hamley and D. K. Smith, *J. Am. Chem. Soc.*, 2008, **130**, 9113-9121; (b) V. J. Nebot, J. Armengol, J. Smets, S. F. Prieto, B. Escuder and J. F. Miravet, *Chem. Eur. J.*, 2012, **18**, 4063-4072.

[20] R. B. Martin, *Chem. Rev.*, 1996, **96**, 3043-3064.

[21] D. H. Zhao and J. S. Moore, *Org. Biomol. Chem.*, 2003, **1**, 3471-3491.

[22] (a) G. Y. Zhu and J. S. Dordick, *Chem. Mater.*, 2006, **18**, 5988-5995; (b) A. R. Hirst and D. K. Smith, *Langmuir*, 2004, **20**, 10851 -10857.

[23] (a) K. Kamiguchi, S. Kuroki, M. Satoh and I. Ando, *Macromolecules*, 2009, **42**, 231-235; (b) P. P. Mitra, P. N. Sen, L. M. Schwartz and P. Ledoussal, *Phys. Rev. Lett.*, 1992, **68**, 3555-3558.

[24] C. S. Johnson, In *Encyclopedia of Nuclear Magnetic Resonance*, vol. 3, Grant DM, Harris RK (eds). John Wiley & Sons: *Chichester*, 1996, 1626-1644.

[25] (a) E. O. Stejskal and J. E. Tanner, *J. Chem. Phys.*, 1965, **42**, 288-292; (b) C. Wende and M. Schonhoff, *Langmuir*, 2010, **26**, 8352-8357.

[26] E. J. Cabrita and S. Berger, *Magn. Reson. Chem.*, 2001, **39**, S142-S148.